PERGAMON

European Journal of Cancer 36 (2000) 2157–2163

European Journal of Cancer

www.ejconline.com

Cell cycle-related expression and ligand binding of peripheral benzodiazepine receptor in human breast cancer cell lines

N. Sänger, R. Strohmeier, M. Kaufmann, H. Kuhl *

Department of Gynecology and Obstetrics, Johann Wolfgang Goethe University, Theodor-Stern Kai 7, 60590 Frankfurt, Germany

Received 8 March 2000; received in revised form 5 June 2000; accepted 8 June 2000

Abstract

The aim of this study was to measure the expression of peripheral benzodiazepine receptors (PBR) as well as mitochondria content in different phases of the cell cycle of BT-20 and MCF-7 breast cancer cell lines, using two-parameter flow cytometric analyses. The PBR expression as well as mitochondria mass, were found to increase as cells pass through different stages of the cell cycle, whereas the amount of PBR in quiescent cells was very low. Binding capacity for the PBR ligand [^{3}H]-Ro5-4864 was strongly related to the phase of the cell cycle with a positive correlation ($r = 0.98$) with a high percentage of cells in S phase. Incubation of BT-20 cells in serum-deprived medium with nanomolar concentrations of Ro5-4864 caused an increase in S phase cells. This effect was not observed in MCF-7 cells. Using micromolar concentrations of Ro5-4864, both BT-20 and MCF-7 cells were reversibly arrested in the $G_{0/1}$ phase.

Keywords: Peripheral benzodiazepine receptors; Cell cycle; Breast cancer cell lines

1. Introduction

Benzodiazepines are widely used drugs in anxiolytic, sedative and muscle relaxant therapy. The binding sites for these drugs are located in the central nervous system, where they interact with the gamma aminobutyric acid receptor (GABA). In addition to these GABA receptor-linked central type of benzodiazepines receptors, a second type has been identified. This peripheral benzodiazepine receptor (PBR) was found throughout the body including the nervous tissue [1–3]. Mostly, PBR was found to be localised in mitochondria, associated with a voltage-dependent anion channel (VADC) and an adenine nucleotide translocater, forming a contact zone between outer and inner mitochondria membranes [4]. Although the exact function of PBRs is still not clear they seem to be involved in steroid genesis [5], immune response [6], and mitochondrial oxidative phosphorylation [7], as well as in the regulation of cell proliferation and tumour growth. Initial studies using high concentrations of drug ligands indicated that their binding to PBR could inhibit DNA synthesis in different kinds of mammalian cell lines [8,9]. Now it has been shown that low concentrations of diazepam, PK 11195 and Ro5-4864 may induce cell proliferation [10,11]. A biphasic effect on cell proliferation depending on the ligand concentration shows that concentrations in the receptor binding range (nanomolar range) stimulate DNA synthesis, whereas PBR ligands are effective as antiproliferative agents in experiments with approximately 1000-fold higher concentrations [8,11,12]. Elevated PBR density was found in several human carcinomas and in some cases PBR expression correlated with tumour malignancy grade and patient survival [13,14]. In addition, in highly aggressive cell lines — relative to non-aggressive cell lines — ligand binding and *PBR*-mRNA was dramatically increased [15]. We found higher PBR expression in faster proliferating oestrogen receptor-negative breast cancer cell lines, than in oestrogen receptor-positive cell lines such as MCF-7 [16].

In this study, we analysed the effects of Ro5-4864 on cell cycle progression. We also investigated the relationship between the expression and binding capacity of PBR in different phases of the cell cycle as well as mitochondria content in the different phases.

* Corresponding author. Tel.: +49-69-6301-5692; fax: +49-69-6301-5522.

E-mail address: h.kuhl@em.uni-frankfurt.de (H. Kuhl).

0959-8049/00/$ - see front matter
PII: S0959-8049(00)00298-7

2. Materials and methods

2.1. Cell culture

The human breast cancer cell lines BT-20, MCF-7, SK-BR3, T47D, BT-474 and MDA-MD-435-S were purchased from the Cell Line Service (CLS, Heidelberg, Germany). Cells were grown in Dulbecco's Modified Eagle's Medium (DMEM, Gibco, Karlsruhe, Germany) supplemented with penicillin/streptomycin (180 IU/ml) in 10% (v/v) fetal calf serum (FCS) and 1% L-glutamine. They were incubated in a humidified atmosphere of 5% CO_2 in air at 37°C. For synchronisation in $G_{0/1}$, semiconfluent cultures were washed with PBS and fresh medium containing 0.5% (v/v) FCS was added. After 48 h when cultures reached a near-quiescent state, culture medium was substituted with DMEM (supplemented with 0.5% (v/v) FCS) containing Ro5-4864 (4′-chlorodiazepam, Fluka Chemie, New-Ulm, Germany) in the concentrations indicated in the results. After 18 h in culture, an analysis of DNA content was carried out. For measurement of the influence of nanomolar and micromolar concentrations of Ro5-4864 on mitochondria mass, cells were grown in DMEM supplemented with 10% FCS and 50 nM or 50 μM Ro5-4865.

2.2. Flow cytometry

For flow cytometry, cells were harvested by trypsinisation, adjusted to 10^6 cells/sample and washed in PBS. For the determination of the cell cycle, cells were fixed in 70% ice-cold ethanol for 10 min, rehydrated in PBS and stained with 10 μg/ml propidium iodide (PI, Sigma-Aldrich, Deisenhofen, Germany). RNAse was added in a final concentration of 0.25 mg/ml. Cell-Fit software (Becton Dickinson, Heidelberg, Germany) was used for data acquisition and determination of cell cycle parameters. The percentage of cells in G_0/G_1, S and $G_{2/M}$ phases of the cell cycle were established on the basis of the corresponding DNA content histograms after exclusion of cell doublets and aggregates.

For PBR levels and mitochondria mass determination, each sample was split into two identical portions of which one was processed for DNA and PBR and the other for DNA and mitochondria. For PBR staining, cells were fixed in 0.4% (w/v) paraformaldehyde in PBS for 5 min. After permeabilisation with a saponin solution (0.1% (w/v) saponin in PBS containing 0.1% (w/v) bovine serum albumin (BSA)) cells were labelled for 30 min at 4°C with 1 μg/ml of the PBR specific MAb 8D7, a kind gift from P. Casellas, Sanofi Recherche, Montpellier, France. Thereafter, cells were washed twice in PBS and resuspended in fluorescein isothiocyanate (FITC)-conjugated goat $F(ab')_2$ antibody to mouse IgG, diluted 100-fold in PBS. Parallel samples were also stained with PI for cell cycle determinations.

For mitochondria labelling, cells were fixed in 70% ice-cold ethanol for 10 min, washed, and rehydrated in PBS. Samples were incubated with 10 μM NAO (10-Nonyl-acredine orange, Molecular Probes, Leiden, The Netherlands) for 15 min at room temperature and washed twice in PBS.

Samples stained for PBR and mitochondria determination were measured on a FACScan (Becton Dickinson) flow cytometer and analysed using Lysis II software. PI fluorescence signal pulse processing (pulse area versus pulse width) was used to exclude doublets and aggregates from analysis. Cells were excited using the 488 nm wavelength of an argon laser. Green and red fluorescence were collected on fluorescence 1 (FL-1) and FL-2 channels, at 530 nm and 585 nm, respectively. The level of background fluorescence, due to the non-specific binding of the FITC-conjugated antibodies was established using control specimens processed as described above, but without exposure to the primary antibodies. 10 000 events were collected in the list mode file for each sample. The relative fluorescence intensity (RFI) was expressed as a multiple of the fluorescence intensity of the control samples. The estimation of PBR expression and mitochondria mass in G_0/G_1, S and $G_{2/M}$ specific cells was done by gating the cells on the basis of DNA content (PI fluorescence, FL-2) and the displaying levels of green fluorescence (FL-1) in the corresponding cell cycle phase after exclusion of doublets (Fig. 1).

Discrimination between G_0 and G_1 cells was achieved by a bivariate analysis of DNA and RNA content based on the use of the metachromic fluorochrome acridine orange (AO, Sigma-Aldrich). 2×10^5 cells in 0.2 ml DMEM containing 10% serum were chilled on ice and 0.4 ml of ice-cold solution A (0.1% Triton X-100, 0.08 N HCl, 0.15 M NaCl) was added, mixed, and further incubated on ice for 15 s. Then 1.2 ml of solution B (6 μg/ml in 1 mM ethylene diamine tetraacetic acid (EDTA) and 150 mM NaCl prepared in phosphate-citric acid butter, pH 6.0) was added to the cells. Control samples containing

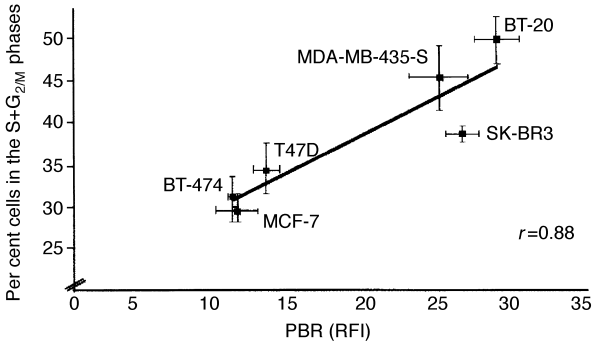

Fig. 1. Correlation between peripheral benzodiazepine receptor (PBR) expression, given as the relative fluorescence intensity (RFI) and percentage of cells in S phase + $G_{2/M}$ of exponentially growing cultures of breast cancer cell lines. Points represent means±standard deviation (S.D.) of six measurements.

50 μg/ml RNase (final concentration) were incubated for 15 min at 37°C. Fluorescence was measured within 2–10 min. The DNA-associated green fluorescence was measured between 515 and 545 nm, and the red luminescence, representing RNA, above 650 nm.

2.3. Binding assay

Cells were harvested and incubated for 40 min at 0°C in a final concentration of 1×10^6 cells/ml in Hank's buffer containing 1.25–20 nM of [^{3}H]-Ro5-4864. Non-specific binding was determined by adding 10 μM unlabelled Ro5-4864. Specific binding was calculated from the difference between total and non-specific binding. Incubation was terminated by transfer of aliquots of radiolabelled cells (1×10^5 cells/0.1 ml) to PBS-prewetted wells of micro-fibre plate (0.65 μm Durapore glass fibre, MultiScreen system, Millipore, Eschborn, Germany) and immediate vacuum filtration. The filters were washed three times with PBS and dried for 5 min at 37°C. Filter discs were punched into vials and radioactivity was counted by liquid scintillation spectrometry (Rackbeta, LKB Wallac, Gottingen, Germany) after incubation for 12 h in scintillation cocktail (Rotiszint, Roth).

The maximal number of binding sites (B_{max}) and equilibrium dissociation constant (K_D) were calculated from saturation curves of [^{3}H]-Ro5-4864 binding, using a Scatchard analysis.

2.4. Statistics

Statistical analysis including the regression line of binding data (Scatchard plot) and Student's *t*-test was carried out using Microsoft Excel.

3. Results

In initial studies, we examined the PBR expression and cell cycle characteristics in exponentially growing cultures of various breast cancer cell lines (BT-20, SK-BR3, MCF-7, T47D, BT-474, MDA-MD-435-S). The cell cycle profile and PBR expression were monitored by flow cytometry of PI and PBR-MAb 8D7-stained cells. To determine the relationship of the proliferating cells and PBR expression, the percentage of cells in the $S+G_{2/M}$ phases was plotted against the RFI of PBR. A regression line for all points gave a coefficient of correlation of (r) 0.88. The results obtained demonstrated that increased expression of PBR correlates with increased numbers of cycling cells (Fig. 1).

BT-20, a cell line with high PBR content, and MCF-7 (low PBR content) were chosen to investigate the relationship between cell cycle phase and PBR expression in more detail. In order to obtain more data on PBR levels in different phases of the cell cycle, cells were PI and PBR MAb 8D7 double-stained and analysed by flow cytometry. Gates were set on the three DNA content regions marked in Fig. 2 and PBR fluorescence examined in each region, i.e. $G_{0/1}$, S phase and $G_{2/M}$. An increasing PBR fluorescence intensity was observed in the S and $G_{2/M}$ phases in both cell lines. PBR expression increased in BT-20 cells from 24.5% (±1.1) in $G_{0/1}$ to 34.0% (±3.0) in S phase and to 41.2% (±2.2) in $G_{2/M}$, while in MCF-7 cells PBR content was lower in $G_{0/1}$ (19.5%) and increased to 48.4% in $G_{2/M}$ (Fig. 3). The

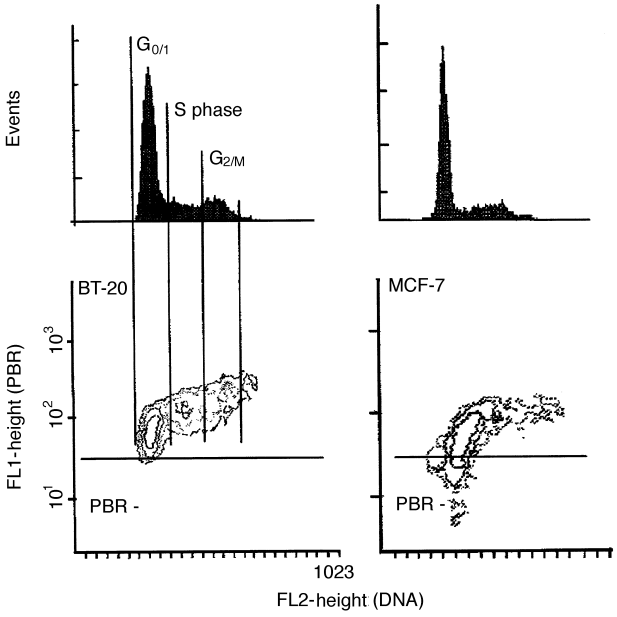

Fig. 2. Two-parameter contour plots, obtained from simultaneous flow cytometric measurements of green fluorescein isothiocyanate (FITC) immunofluorescence with anti-peripheral benzodiazepine receptor (PBR) antibody and red propidium iodide (PI) fluorescence of BT-20 and MCF-7 cells, showing the distribution of PBR in relation to the cell cycle phase. Distinction between the different phases of the cell cycle was done by setting gates based on DNA content from DNA histograms as indicated by vertical lines. The horizontal lines indicate the threshold of PBR-negative and -positive cells.

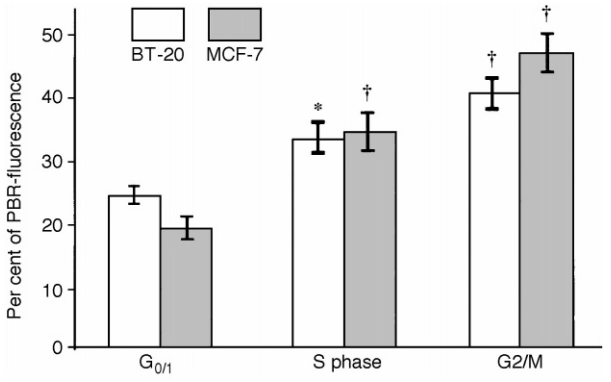

Fig. 3. Peripheral benzodiazepine receptor (PBR) levels in the different phases of the cell cycle in BT-20 and MCF-7 cells grown in 10% fetal calf serum (FCS). Each bar represents the mean±standard deviation (S.D.) of six separate measurements (see Fig. 1.). *$P<0.01$, †$P<0.001$.

PBR levels were most variable during the $G_{0/1}$ phase of MCF-7 cells. 20–25% of $G_{0/1}$ cells were weakly stained or PBR-negative as seen by fluorescence intensity (Fig. 1), thereby implying that the lowest levels of PBR are associated with a subpopulation of $G_{0/1}$ cells. In the S and $G_{2/M}$ phases approximately 97% of all cells were PBR-positive. In BT-20 cells, the PBR-negative subpopulation was very small (<2%) in exponentially growing cell cultures. After 48 h of serum deprivation however, when approximately 85% of the BT-20 cells were in $G_{0/1}$, up to 35% of the cells were PBR-negative or weakly stained (data not shown).

To make a distinction between quiescent cells (G_0) and active cells in the $G_{0/1}$ phase of the cell cycle, we measured the DNA/RNA contents of the cells by acridine orange staining. Two typical patterns of RNA/DNA distribution in proliferating cells and in cells after 48 h of serum deprivation are shown in Fig. 4. In BT-20 cell cultures containing approximately 65% cells in $G_{0/1}$ 13.16% (±0.79) were RNA-negative or weakly stained and this proportion increased to 55.12% (±1.57) when $G_{0/1}$ cells increased to approximately 85% after serum deprivation. Cells lost 21.41% (±0.98) of the total RNA fluorescence measured in exponentially growing cultures. In MCF-7 cells, the proportion of RNA-negative cells was higher in asynchronously growing cells (16.63%±2.4) and only increased to 34.76% (±1.36) after serum deprivation (data not shown).

The results from the PBR measurements are in good accordance with binding experiments. The binding capacity of BT-20 cells for [^{3}H]-Ro5-4864 was strongly related to cell cycle phases with a negative correlation ($R = -0.98$) to the percentage of cells in $G_{0/1}$ and a positive correlation ($r = 0.98$) to cells in S phase (Table 1). These experiments were not carried out with MCF-7 cells because of their very low binding capacity [15,16].

Table 1
Scatchard analysis of [^{3}H]-Ro5-4864 binding of BT-20 cells in various states of the cell cycle

[^{3}H]-Ro5-4864 binding		Cell cycle phase		
B_{max} fM/10^6 cells	K_D nM	$G_{0/1}$ % cells	S phase % cells	$G_{2/M}$ % cells
231.4	5.6	93	3	4
302.9	10.1	90	7	3
355.4	5.0	74	21	5
374.1	8.2	68	25	7
382.1	8.9	67	25	8
587.3	10.6	23	75	2
784.8	11.1	8	90	2

B_{max}, maximal number of binding sites; K_D, equilibrium dissociation constant.

As the PBR is located in the mitochondria membrane, we also analysed the mitochondria mass in the different cell cycle phases by two-parameter flow cytometry. PI staining was used for DNA content determination and NAO (a specific dye for the assessment of mitochondrial membrane mass) for mitochondria. DNA content was used to separate the various cell cycle compartments and NAO fluorescence was determined in $G_{0/1}$, S phase and $G_{2/M}$ cells. Mitochondria content increased continuously as the cells passed through the cell cycle in BT-20 cells (Fig. 5), as well as in MCF-7 cells (data not shown). Mitochondria mass increased by 23% (±3) in S

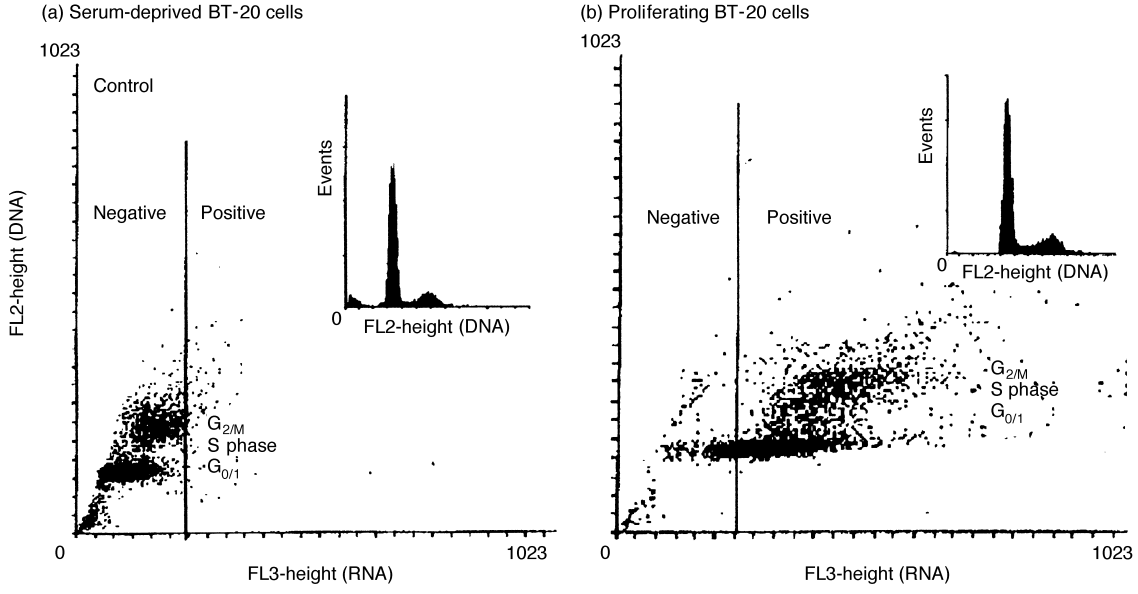

Fig. 4. DNA and RNA distribution in (a) serum-deprived BT-20 cells and (b) proliferating BT-20 cells grown in medium containing 10% fetal calf serum (FCS). The cells were stained with propidium iodide (PI) (DNA = y axis) and acridine orange (RNA = x axis). The distinction between positive and negative cells was based on the RNAse-treated control samples. The threshold between negative and positive cells is indicated by a vertical line. The inserts show the corresponding DNA histograms.

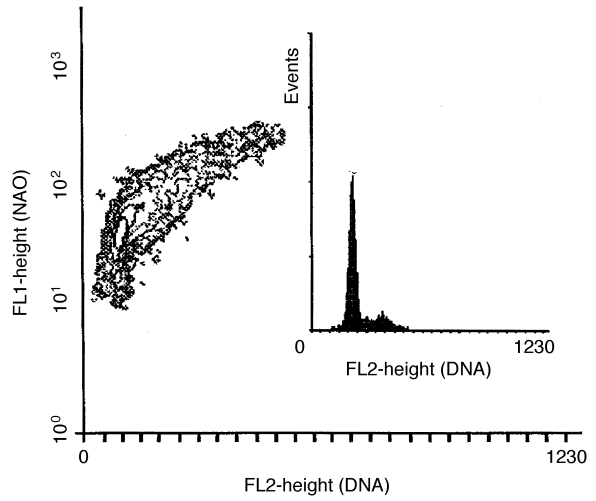

Fig. 5. Two-parameter contour plot of simultaneous flow cytometric measurements of propidium iodide (PI) (DNA = x axis) and nonyl-acredine orange (mitochondria = y axis) stained BT-20 cells, showing the increase of mitochondria fluorescence with an increase in DNA fluorescence. The insert shows the corresponding DNA histogram.

phase and by 50% (±3.7) in $G_{2/M}$ compared with $G_{0/1}$ in BT-20 cells. As expected, no negative cells were found (Fig. 5). Incubation of the cells with 50 nM Ro5-4865 for 4 h led to increased proportions of PBR, as well as of mitochondria mass. The rise in total PBR expression (65.85%±10) was approximately twice that in mitochondria (36.5%±2). 50 μM of Ro5-4865 caused a reduction in PBR (31.5%±3), whereas the mitochondrial mass remained at the same level as in untreated cells.

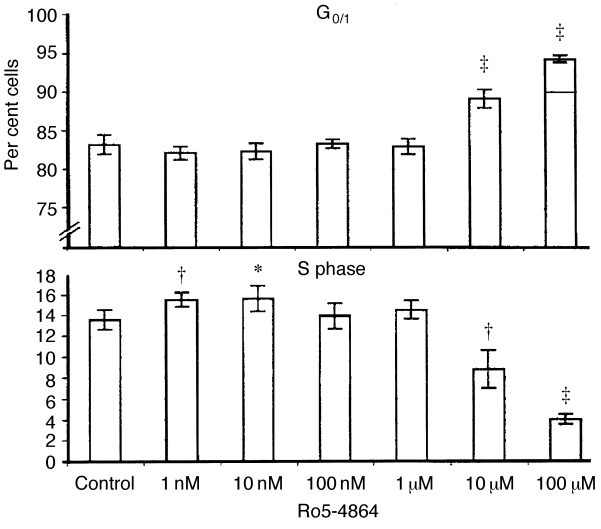

Fig. 6. Dose–response effect on BT-20 cell cycle phase distribution after the addition of Ro5-4864. Cells were seeded at 5×10^5 cells/100 mm^2 plastic dishes in Dulbecco's Modified Eagle's Medium (DMEM) (10% fetal calf serum (FCS)) overnight, serum-starved (0.5% FCS) for 48 h and further incubated in the presence of the indicated concentrations of Ro5-4864 in serum-free medium (0.5% FCS) for 18 h. Each bar represents the mean±standard deviation (S.D.) of two separate experiments run in triplicate. *$P<0.05$; †$P<0.01$; ‡$P<0.001$.

The effects of Ro5-4864 on the progression of synchronised BT-20 cells through the cell cycle are shown in Fig. 6. Ro5-4864 was added after 48 h of serum deprivation, when approximately 85% of all cells were in $G_{0/1}$. The cultures were incubated for 18 h in culture medium without serum (i.e. 0.5% FCS) containing the indicated drug concentrations before analysis of the cellular DNA content. Micromolar Ro5-4864 concentrations (10–100 μM) resulted in an increased proportion of cells in $G_{0/1}$ and a corresponding reduction in the numbers entering S phase. In contrast, nanomolar concentrations (1–10 nM) caused an increased percentage of cells in S phase. However, MCF-7 cells showed no significant increase in S phase when incubated with nanomolar Ro5-4864 concentrations, while micromolar concentrations also led to a cell cycle arrest in $G_{0/1}$ (data not shown). The inhibitory effect of Ro5-4864 in the micromolar range was fully reversible after addition of culture medium (containing 10% FCS) in both cell lines (data not shown).

4. Discussion

In this study, the PBR expression as well as mitochondrial mass, were found to increase as cells pass through different stages of the cell cycle. Concomitantly, binding of the PBR ligand Ro5-4864 increases according to PBR expression.

The two-colour flow cytometric assays revealed that expression of PBR increases in a near-linear fashion during the course of the cell cycle of MCF-7 and BT-20 cells. In S and $G_{2/M}$ phases, PBR distribution was found to be homogeneous in all cells. A more heterogeneous distribution of staining intensity was found in $G_{0/1}$ cells. The heterogeneity reflected the presence of both cells with no or very low levels of PBR and cells with higher levels. As the percentage of PBR-negative cells increased with increasing proportions of cells with very low RNA content, which are regarded as quiescent cells (G_0) [17], PBR appeared to be downregulated in this cell population. These findings are in agreement with results from primary astrocytes and C6 glioma cells, where the highest immunoreactivity for PBR was observed in dividing cells, while in confluent cell layers the staining intensity was significantly decreased [18]. In C6 glioma cells, a decrease of specific PK11195 binding after preincubation with serum-free medium was observed [10].

Similar to PBR, a near-linear increase was found in mitochondrial mass during the cell cycle.

While the PBR is predominantly localised in the mitochondrial membrane [19], a few reports describe additional benzodiazepine binding sites in other intracellular locations, e.g. the nucleus, Golgi, lysosomes and peroxisomes [20]. Recently, Hardwick and colleagues [15] found PBR in aggressive metastatic breast tumour

biopsies, as well as in highly aggressive cell lines localised primarily in and around the nucleus. We previously reported a correlation of PBR expression and mitochondria mass in several breast cancer cell lines [16]. In this study, the same monoclonal antibody to the C-terminal fragment of the human PBR [21] was used and cellular localisation studies by confocal microscopy showed that the antibody is colocalised exclusively with mitochondria and did not react with the plasma membrane or other organelles [16,21]. This does not mean that there are no PBRs in other compartments of the cell, but it is possible that this antibody could simply not recognise any other form of PBR due to a slight difference in conformations of the receptor's C-terminus.

Some years ago, a near-linear synthesis of mitochondrial mass over the cell cycle was described in HL-60 human leukaemia cells using rhodamine 123 (RH 123) as a fluorescence dye [22]. In the meantime, RH 123 uptake was shown to be driven by the mitochondrial membrane potential and may indicate mitochondrial function rather than mitochondrial mass [23]. The dye used in this study, nonyl-acridine orange, is a newer compound [24] that freely diffuses into cells and binds to cardiolipin in the mitochondrial membrane, giving a fluorescence staining that is independent of mitochondria activity. However, Leprat and associates [24] found a correlation between NAO, RH 123 uptake and DNA content during the cell cycle concluding that there is an increase in mitochondrial mass, as well as in mitochondrial function, while cells pass through the cell cycle. In C6 and T98G glioma cells, benzodiazepine induced proliferation of mitochondria. As shown by quantitative electron microscopy, 10 nM of Ro5-4865 caused a 2.5 times increase in the number of mitochondria compared with cells incubated in serum-free medium [25]. This increase which is much higher than that observed in BT-20 or MCF-7 cells, may be due to differences in the methods employed and cell type.

The effect of starving is a reduction in protein synthesis leading to cell cycle arrest at the restriction point in mid-G_1 and eventual withdrawal into a G_0 resting state. As we found RNA-positive as well as RNA-negative cells in the $G_{0/1}$ fraction of serum-starved cells, we assume that cells in G_1 are able to go on through the cell cycle and accumulate in G_0 after mitosis despite the presence of micromolar concentrations of Ro5-4864. However, nanomolar concentrations of Ro5-4864 stimulate BT-20 cells to exit $G_{0/1}$ and enter S phase even without the addition of serum. The biphasic response of BT-20 cells was also shown in cells grown with optimal serum concentrations (10% FCS) by [^{3}H]-thymidine incorporation experiments [11]. The reversibility of the inhibitory effect as well as the completion of the cell cycle in the presence of micromolar concentrations of Ro5-4864 shows that even high concentrations must not be cytotoxic.

The physiological role of PBR is still debated. Its major function in endocrine tissues and some cell lines seems to be associated with cholesterol transport and steroidogenesis (reviewed in [5]). However, there are tissues and cells lines where PBR is expressed, but no steroid synthesis takes place. Therefore, various functions of PBR may be assumed in different tissues. PBR expression also correlates with the proportion of proliferating cells [16] and tumour malignancy [13,14,26] which is associated with a rise in the proliferative index. As energy requirements are higher in growing cells, higher expression of PBR might be an indicator of increased metabolic activity in malignant cells. An endogenous ligand of the PBR, the diazepam binding inhibitor (DBI) may have an important role in insect energy metabolism and is expressed mainly in cell types catabolising fatty acids as a primary substrate for energy production [27]. Acyl-CoA binding protein of rat liver, which is identical with DBI of the rat brain, was shown to take part in acyl-CoA transport and pool forming and seems to be able to stimulate mitochondrial acyl-CoA synthetase and to transport it for mitochondrial β-oxidation [28]. An involvement of PBR in energy generation, which is important for all aspects of cell metabolism, may explain its higher expression during the active phases of the cell cycle and fast growing aggressive tumours.

Acknowledgements

We thank Manfred Stegmüller for technical advice with the flow cytometer.

References

1. DeSouza EB, Anholt RRH, Murphy KWM, Snyder SH. Peripheral-type benzodizepine receptor in endocrine organs: autoradiographic localization in rat pituitary, adrenal and testis. *Endocrinology* 1985, **116**, 567–573.
2. Fares FA, Gavish M. Characterization of peripheral benzodiazepine binding sites in human term placenta. *Biochem Pharmacol* 1986, **35**, 227–230.
3. Gehlert DR, Yamamura H, Wamsly JK. Autoradiographic localization of "peripheral" benzodiazepine binding sites in rat brain and kidney. *Eur J Pharmacol* 1985, **95**, 329–330.
4. McEnery MW, Snowman AM, Trifiletti RR, Snyder SH. Isolation of the mitochondrial benzodiazepine receptor: association with the voltage dependent anion channel and the adenine nucleotide carrier. *Proc Natl Acad Sci USA* 1992, **89**, 3170–3174.
5. Papadopoulos V, Amri H, Boujrad N, *et al*. Peripheral benzodiazepine receptor in cholesterol transport and steroidogenesis. *Steroids* 1997, **62**, 21–28.
6. Taupin V, Herbelin A, Descamps-Latscha B, Zavala F. Endogenous anxiogenic peptide, ODN-diazepam binding inhibitor, and benzodiazepines enhance the production of interleukin-1 and tumor necrosis factor by human monocytes. *Lymphokine Cytokine Res* 1991, **10**, 7–13.

7. Carayon P, Portier M, Dussossoy D, *et al*. Involvement of peripheral benzodiazepine receptors in the protection of hematopoietic cells against oxygen radical damage. *Blood* 1996, **87**, 3170–3178.
8. Wang JKT, Morgan JI, Spector S. Benzodiazepines that bind at peripheral sites inhibit cell proliferation. *Proc Natl Acad Sci USA* 1984, **81**, 753–756.
9. Clarke GD, Ryan PJ. Tranquillizers can block mitogenesis in 3T3 cells and induce differentiation in Friend cells. *Nature* 1980, **287**, 160–161.
10. Ikezaki K, Black KL. Stimulation of cell growth and DNA synthesis by peripheral benzodiazepine. *Cancer Lett* 1990, **49**, 115–120.
11. Beinlich A, Strohmeier R, Kaufmann M, Kuhl H. Specific binding of benzodiazepines to human breast cancer cell lines. *Life Sci* 1999, **56**, 2099–2108.
12. Carmel I, Fares FA, Leschiner S, Scherübl H, Weisinger G, Gavish M. Peripheral-type benzodiazepine receptors in the regulation of proliferation in MCF-7 human breast carcinoma cell line. *Biochem Pharmacol* 1999, **58**, 273–278.
13. Katz Y, Ben-Baruch G, Kloog Y, Menczer J, Gavish M. Increased density of peripheral benzodiazepine-binding sites in ovarian carcinomas as compared with benign ovarian tumours and normal ovaries. *Clin Sci* 1990, **78**, 155–158.
14. Mietttinen H, Kononen J, Haapasalo H, *et al*. Expression of peripheral-type benzodiazepine receptor and diazepam binding inhibitor in human astrocytomas: relationship to cell proliferation. *Cancer Res* 1995, **55**, 2691–2695.
15. Hardwick M, Fertikh D, Culty M, Li H, Vidic B, Papadoloulos V. Peripheral-type benzodiazepine receptor (PBR) in human breast cancer: correlation of breast cancer cell aggressive phenotype with PBR expression, nuclear localization, and PBR-mediated cell proliferation and nuclear transport of cholesterol. *Cancer Res* 1999, **59**, 831–842.
16. Beinlich A, Strohmeier R, Kaufmann M, Kuhl H. Relation of cell proliferation to expression of peripheral benzodiazepine receptors in human breast cancer cell lines. *Biochem Pharmacol* 2000, in press.
17. Crissman HA, Darzynkiewicz Z, Tobey RA, Steinkamp JA. Correlated measurements of DNA, RNA and protein in individual cells by flow cytometry. *Science* 1985, **288**, 1321–1324.
18. Alho H, Varga V, Krueger KE. Expression of mitochondrial benzodiazepine receptor and its putative endogenous ligand diazepam binding inhibitor in cultured primary astrocytes and C-6 cells: relation to cell growth. *Cell Growth Different* 1994, **5**, 1005–1014.
19. Krueger KE, Papadopoulos V. Peripheral-type benzodiazepine receptors mediate translocation of cholesterol from outer to inner mitochondrial membranes in adrenocortical cells. *J Biol Chem* 1990, **265**, 15015–15022.
20. O'Beirne GB, Woods MJ, Williams DC. Two subcellular locations for peripheral-type benzodiazepine acceptors in rat liver. *Eur J Biochem* 1990, **188**, 131–138.
21. Dussossoy D, Carayon P, Feraut D, *et al*. Development of a monoclonal antibody to immuno-cytochemical analysis of the cellular localization of the peripheral benzodiazepine receptor. *Cytometry* 1996, **24**, 39–48.
22. James TW, Bohman R. Proliferation of mitochondria during the cell cycle of the human cell line (HL-60). *J Cell Biol* 1981, **89**, 256–260.
23. Freyer JP. Decreased mitochondrial function in quiescent cells isolated from multicellular tumor spheroids. *J Cell Physiol* 1998, **176**, 138–149.
24. Leprat P, Ratinaud MH, Maftah A, Petit JM, Julien R. Use of nonyl acredine orange and rhodamine 123 to follow biosynthesis and functional assembly of mitochondrial membrane during L1210 cell cycle. *Exp Cell Res* 1990, **186**, 130–137.
25. Shiraishi T, Black KL, Ikezaki K, Becker DP. Peripheral benzodiazepine induces morphological changes and proliferation of mitochondria in glioma cells. *J Neurosci Res* 1991, **3**, 463–474.
26. Venturini I, Alho H, Podkletnova I, *et al*. Increased expression of peripheral benzodiazepine receptors and diazepam binding inhibitor in human tumors sited in the liver. *Life Sci* 1999, **65**, 2223–2231.
27. Kolmer M, Roos C, Tirronen M, Myöhänen S, Alho H. Tissue-specific expression of the diazepam-binding inhibitor in *Drosophila melanogaster*: cloning, structure, and localization of the gene. *Mol Cell Biol* 1994, **14**, 6983–6995.
28. Knudsen J, Mandrup S, Rasmussen JT, Andreasen PH, Poulsen R, Kristiansen K. The function of acyl-CoA-binding protein (ACBP)/diazepam binding inhibitor (DBI). *Mol Cell Biochem* 1993, **123**, 129–138.